An Assessment of Low-Frequency Variability in the Tropics as Indicated by Some Proxies of Tropical Convection

PRASHANT D. SARDESHMUKH AND BRANT LIEBMANN

Cooperative Institute for Research in the Environmental Sciences, University of Colorado, Boulder, Colorado

(Manuscript received 25 September 1991, in final form 29 May 1992)

ABSTRACT

Any discussion of intraseasonal and interannual variability in the atmosphere must presume a reliable assessment of the observed variability. In spite of continued improvements in observing systems, quality control techniques, and data analysis schemes, however, and also because of them, this assessment remains difficult in the tropics.

In this paper the authors examine the mean tropical circulation during two Januarys, 1988 and 1989, as described by the circulation analyses produced at two weather prediction centers, the National Meteorological Center (NMC) in Washington, D.C., and the European Center for Medium-Range Weather Forecasts (ECMWF) in Reading, England. In particular, the authors' focus is on the *change* in the circulation between 1988 and 1989 as estimated by these two sets of analyses, especially the change in the 200-mb wind divergence associated with organized deep convection. The authors find that in many regions the discrepancy between these estimates is of the order of the change itself. A comparison with maps of the outgoing longwave radiation (OLR) is not quantitatively useful in this regard.

One way out of this dilemma is to derive divergence fields that are consistent with the 200-mb vorticity balance. The authors do so by solving the "chi problem" of Sardeshmukh and Hoskins. Because the large-scale vorticity fields generated by NMC and ECMWF are highly correlated (~98%), the divergence fields derived in this manner are also better correlated than the analyzed fields and enable a more reliable assessment of the observed change between these two periods.

1. Introduction

In this paper we will assess the ability of the routine circulation analyses produced at operational weather forecasting centers to represent low-frequency variability in the tropics. Lack of adequate observations, differences in quality control procedures, differences in models used to provide background fields for the data analysis, and differences in analysis schemes all contribute to the perceived difference between the analyzed circulation patterns. We will not provide an exhaustive documentation of these differences here, or the reasons for their existence. Our main interest is in examining their magnitude relative to the magnitude of intraseasonal and interannual circulation changes. Similar magnitudes would clearly give cause for concern, but as we will see, this is unfortunately the case for some dynamically important quantities. We will then develop a procedure to alleviate the problem.

For brevity we will restrict ourselves to a discussion of the 200-mb flow. Teleconnections between different tropical regions and between the tropics and middle latitudes are most evident at upper-tropospheric levels, and the horizontal wind divergence at these levels is closely associated with tropical convection. We will consider the analyses produced at two centers, the National Meteorological Center (NMC) in Washington, D.C., and the European Centre for Medium-Range Weather Forecasts (ECMWF) in Reading, England. Finally, we will select two periods, January 1988 and January 1989, for detailed study.

Figure 1a shows the January 1988 mean relative vorticity $\xi = \mathbf{k} \cdot \nabla \times \mathbf{v} = \nabla^2\psi$ of the 200-mb flow as analyzed at NMC. As with all the other maps in this paper, the figure shows the tropical portion of a global field truncated at total wavenumber 12. Instead of showing the corresponding ECMWF (EC) field, which looks very similar, we show the difference ξ(NMC) − ξ(EC) in Fig. 1b. We will show such maps throughout the paper to highlight the difference between the NMC and EC fields. We will also interpret them as indicative of the uncertainty in the analyzed fields.

The values in Fig. 1b are clearly much smaller than in Fig. 1a; thus, the NMC and EC vorticity fields show a high degree of consistency. Figure 2 shows that this is also true of the estimates of interannual change. Figure 2a shows $\Delta\xi$(NMC), the change in the vorticity between January 1988 and January 1989. The difference between it and the corresponding EC field is given in Fig. 2b. Again, this is much smaller than $\Delta\xi$.

As we shall see in Figs. 5 and 6, the same consistency does not obtain for the estimates of the horizontal wind divergence $D = \nabla \cdot \mathbf{v} = \nabla^2\chi$. Sardeshmukh and Hoskins

Corresponding author address: Prashant D. Sardeshmukh, University of Colorado, Campus Box 449, Boulder, CO 80309.

(1987; hereafter SH) proposed to improve upon such a situation by diagnosing the divergence from the vorticity budget

$$\partial\zeta/\partial t + \mathbf{v}_\psi \cdot \nabla\zeta + \nabla\cdot(\zeta\nabla\chi) - F = -C = 0. \quad (1)$$

Here $\zeta = \xi + f = \mathbf{k}\cdot\nabla\times\mathbf{v}_\psi + f$ is the absolute vorticity, χ is the velocity potential, and F represents vertical advection, twisting, and frictional terms. If one specifies the rotational flow and its tendency in Eq. (1), and also F in terms of the horizontal flow, then one can solve for the velocity potential χ. This is the so-called chi problem. If the vorticity fields are reliable, then one expects that the divergence fields derived in this manner will also be reliable. We shall construct such divergence fields here and call them *Dchi* to distinguish them from the analyzed divergence fields D.

The paper is organized as follows. The method of solving (1) is outlined in section 2. This is a refinement of the iterative approach followed by SH and is discussed in depth in a companion paper by Sardeshmukh (1993). The technical details are not repeated here. In section 3 five different estimates of the January 1988 200-mb divergence fields are presented: D(NMC), D(EC), *Dchi*(NMC), *Dchi*(EC), and outgoing longwave radiation (OLR). In section 4 the changes Δ in these fields between 1988 and 1989 are presented in an identical format. A case is made that the *Dchi* and Δ*Dchi* fields represent an improvement over the analyzed D and ΔD fields, and enable a more consistent description of interannual variability. The mean meridional circulation is discussed in section 5, and a summary and directions for future work follow in section 6.

2. Method of solving the chi problem

As in SH an iterative approach to the solution of Eq. (1) is followed, making successive refinements to the divergence D until the vorticity budget residual C becomes small. New guesses are generated by applying the formula

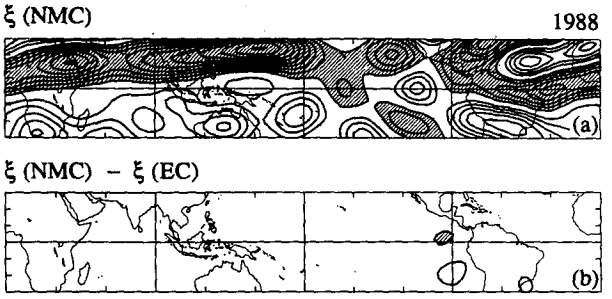

FIG. 1. The NMC analysis of the January 1988 mean relative vorticity at 200 mb and the difference between it and the corresponding ECMWF analysis. Positive values are indicated by solid and negative by shaded contours. The zero contour is not shown. The contour interval is 5×10^{-6} s^{-1} in both panels. Lines of latitude and longitude are drawn every 90 degrees. Tick marks are also shown along the edges for every 30 degrees of longitude and 10 degrees of latitude.

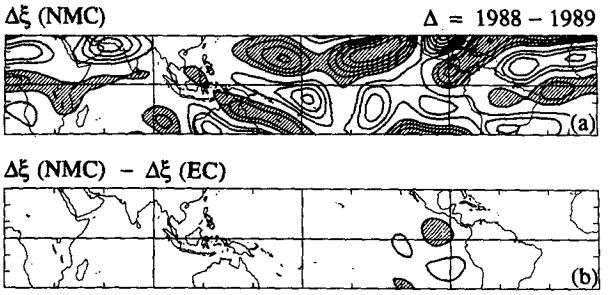

FIG. 2. As in Fig. 1 but for the January 1988 minus January 1989 difference.

$$D_{l+1} = D_l + 2\alpha\nabla^{-2}\{\nabla\cdot(\zeta\nabla\epsilon C_l)\}. \quad (2)$$

Here l is the iteration index, $\epsilon = 1/(\zeta^2 + 4\Omega^2\mu_0^2)$, and α, Ω, and μ_0 are constants, with values $\alpha \sim 0.5$, $\Omega = 7.292\times10^{-5}$ s^{-1}, and $\mu_0 \sim 0.6$. The inverse Laplacian operator ∇^{-2} is such that if $x = \nabla^2 y$, then $y = \nabla^{-2}x$.

The basis for such an iteration formula is the following. Consider the number $G = \langle \epsilon C^2\rangle$, where C and ϵ are as defined above and angle brackets denote a global integral. Basically, ϵ is chosen to give greater weight to tropical regions. Note that G is positive, and a necessary and sufficient condition for C to be zero everywhere is that G is zero. It can be shown, through repeated integration by parts, that a small arbitrary change δD in D implies a change δG in G given by $\delta G = -\langle\nabla^{-2}[\nabla\cdot(\zeta\nabla 2\epsilon C)]\delta D\rangle$. If we choose $\delta D = \alpha\nabla^{-2}[\nabla\cdot(\zeta\nabla 2\epsilon C)]$, where α is a positive constant, then δG will be negative, and G, and therefore C, will decrease. This leads immediately to (2).

In essence, at each iteration δD is chosen to lie down the gradient of G with respect to the divergence field. Our choice of ϵ is such as to make that gradient approximately the same in all directions. Thus, our iteration formula has some advantages over that used by SH. It guarantees that the iteration will converge to the solution $C = 0$ for a small enough α, and because of the choice of ϵ, also gives a faster approach to the solution in the tropics. As in SH, we start the iterations with the analyzed divergence fields as the first guess.

The time-averaged version of (1) reads

$$\overline{\partial\zeta/\partial t} + \mathbf{v}_\psi\cdot\nabla\zeta + \nabla\cdot(\zeta\nabla\chi) + \nabla\cdot\overline{(\mathbf{v}'\zeta')} - F = 0. \quad (3)$$

An overbar here denotes a monthly mean and a prime a deviation from it. All other quantities in this equation are monthly means, the bar over them having been dropped for convenience. We ignore the tendency term and F, and specify the transient eddy term from the daily analyses. This as well as the vorticity advection by the mean rotational wind are kept fixed when iterating (2).

The calculation is performed on the sphere by expanding all fields in a series of spherical harmonics

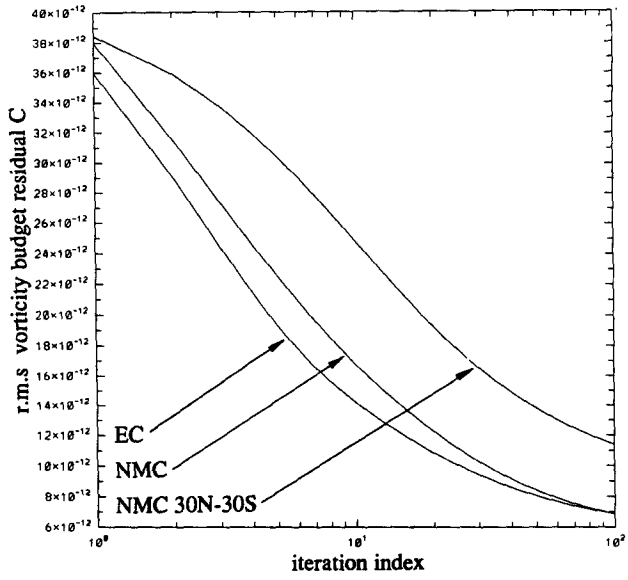

FIG. 3. The global root-mean-square vorticity budget residual C in units of s^{-2} as a function of the iteration employed for solving the chi problem. The '30–30' curve refers to the rms of C in the tropical belt 30°N–30°S.

truncated at total wavenumber $n = 24$. However, we attempt to balance the vorticity budget only for total wavenumbers 1 through 12. It is assumed that the budget residual on these scales arises entirely from errors in the wavenumbers 1 through 12 of the divergence. Thus, only these components of D are updated by formula (2). In the terminology of SH, this corresponds to $N = 24$ and $N' = 12$.

Figures 3 and 4 give an indication of the performance of the technique. Figure 3 shows that the global root-mean-square (rms) of C decreases smoothly to less than half its initial value in 10 iterations. The decrease thereafter is considerably slower. Also, C shows a slower decrease in the tropics than elsewhere. This is evident in the maps of C after 100 iterations, given in Fig. 4. Nevertheless, the reduction in C almost everywhere after only 100 iterations is significant, and considering the uncertainties in the formulation of F, is reasonably satisfactory.

We have attempted to solve (1) by standard conjugate gradient methods. In the few cases examined the convergence rate was slower than in Fig. 3 and the decrease of C was erratic. Our present view is that the relatively small values of both the absolute vorticity and the absolute vorticity gradient in the tropics make this problem less tractable by standard techniques, and that some tuning is required to make them work.

3. Divergence fields for January 1988

Five different estimates of the January mean 200-mb divergence are discussed herein: D(NMC), D(EC), *Dchi*(NMC), *Dchi*(EC), and OLR. Note that *Dchi*(NMC) and *Dchi*(EC) are obtained using the NMC and EC vorticity fields, respectively. As in section 1, we actually show D(NMC) − D(EC) and *Dchi*(NMC) − *Dchi*(EC) in Fig. 5 to highlight the difference between the NMC and EC fields. Also, instead of OLR we actually show MOLR = 255 − OLR, where OLR is in Watts m^{-2}. Thus, positive values of MOLR (i.e., OLR less than 255 Watts m^{-2}) indicate upper-level divergence, and negative values of MOLR indicate upper-level convergence.

The comparison between D(NMC) and MOLR for January 1988 is good in a gross sense. Both fields indicate local heating maxima over southern Africa, the east Indian Ocean, the central Pacific Ocean, and the Amazon Basin. The maxima in D(NMC) over the western Indian Ocean and the extreme western Pacific Ocean north of Darwin, however, have no corresponding features in the MOLR field. Also, D(NMC) shows considerably greater structure than MOLR in the areas of upper-level convergence, but this is perhaps to be expected.

The discrepancy between D(NMC) and D(EC) is given in the map of D(NMC) − D(EC). There are significant differences over Africa and the Amazon Basin, and to a lesser extent over the central Pacific. Interestingly, the differences are not large over the southwest Indian and the extreme western Pacific oceans, two areas in which the correspondence between D(NMC) and MOLR is poor. Thus, although the NMC and EC analyses are mutually consistent here, they are both inconsistent with MOLR.

The chi problem solution *Dchi*(NMC) shows a somewhat better agreement with MOLR in convective areas. In particular it shows reduced values over the

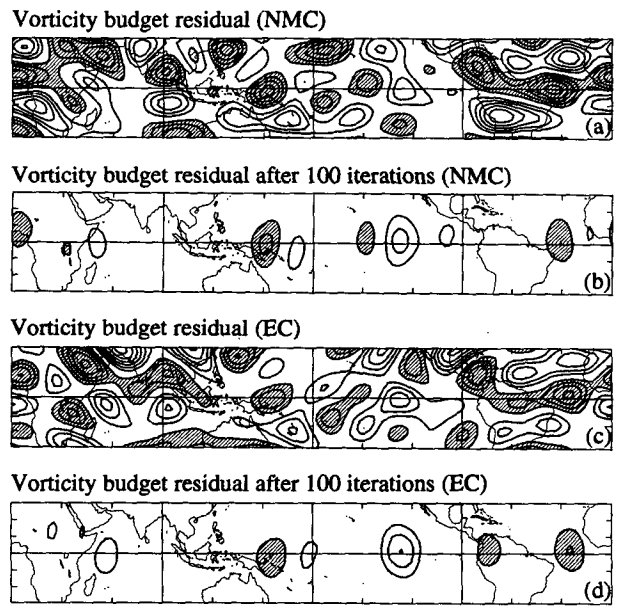

FIG. 4. (a) The vorticity budget residual C for January 1988 computed using the NMC analyses. (b) The same field after 100 iterations of the chi problem. (c) and (d) As in (a) and (b) but using the ECMWF analyses. Contouring convention as in Fig. 1 except the contour interval is 2×10^{-11} s^{-2}.

southwest Indian and extreme western Pacific oceans. The difference map *Dchi*(NMC) − *Dchi*(EC) also shows generally smaller values than *D*(NMC) − *D*(EC), indicating a greater consistency between the chi problem solutions than between the analyzed fields.

The MOLR field (Fig. 5e) is useful for delineating the areas of deep convection. A quantitative link between its values and those of the upper-level divergence is tempting to establish but has remained elusive. Julian (1984) proposed a scheme for tropical wind analysis that takes the OLR information into account. Results from several studies indicate that the temporal correlation of monthly mean OLR and the upper-level divergence is of order −0.6. The spatial correlation is probably higher in the convective areas. Thus, even though we do not know quite what to make of the numerical values of OLR, we believe its spatial structure in the areas of convection. For example, we believe that during January 1988 there was relatively less convective activity over the southwest Indian and extreme western Pacific oceans than over the central Pacific Ocean.

4. Estimates of the 1988–1989 difference

Figure 6 shows estimates of the difference between the January 1988 and January 1989 fields in a format identical to that of Fig. 5. As in section 1, the symbol Δ always refers to this difference. The difference in the NMC divergence is given in the map of Δ*D*(NMC). The discrepancy between this and the corresponding EC field is given in the map of Δ*D*(NMC) − Δ*D*(EC). These maps show that in many regions the discrepancy between the NMC and EC estimates of the 1988–1989 change is of the order of the change itself, in striking contrast with the estimates of the vorticity change presented in Fig. 2.

When the chi problem solutions are used to estimate the change, the situation is improved. The values of Δ*Dchi*(NMC) − Δ*Dchi*(EC) are generally smaller than those of Δ*Dchi*(NMC). However, there remain some areas, such as East Africa and the Amazon Basin, where there is no improvement. We will return to this point.

Figure 6 also shows the difference in the MOLR between 1988 and 1989. The correspondence between the divergence and the MOLR fields is poorer than in Fig. 5. There is considerably more structure in the Δ*D* and Δ*Dchi* fields than in ΔMOLR. For example, the positive values in the central Pacific are split into two centers in both Δ*D* and Δ*Dchi*, whereas ΔMOLR shows a single broad maximum. Farther west, ΔMOLR indicates strong anomalous convergence to the north of New Guinea, but the corresponding feature in the Δ*D* and Δ*Dchi* fields is relatively weak; ΔMOLR misses most of the structure over the central north and eastern Pacific Ocean.

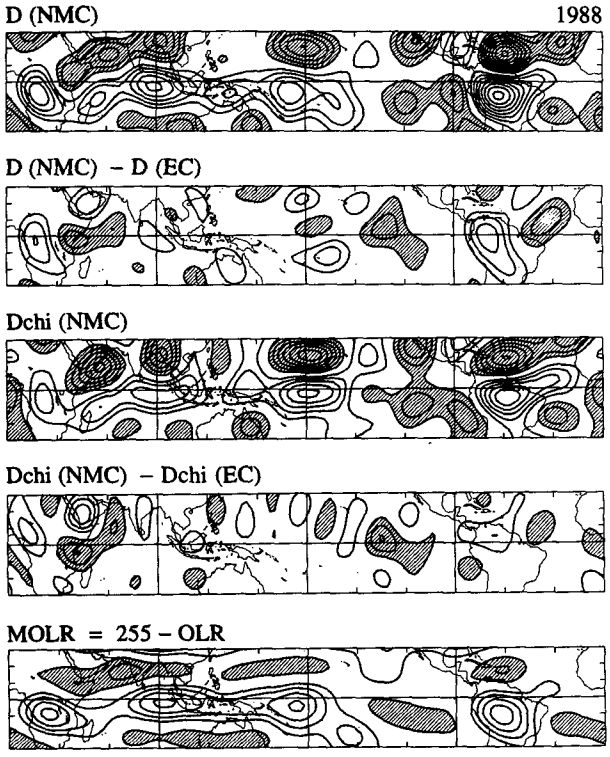

FIG. 5. Divergence and MOLR fields for January 1988. See text for full explanation. The contour interval is 1×10^{-6} s^{-1} for the divergence and 15 Watts m^{-2} for MOLR; otherwise the contouring convention is as in Fig. 1.

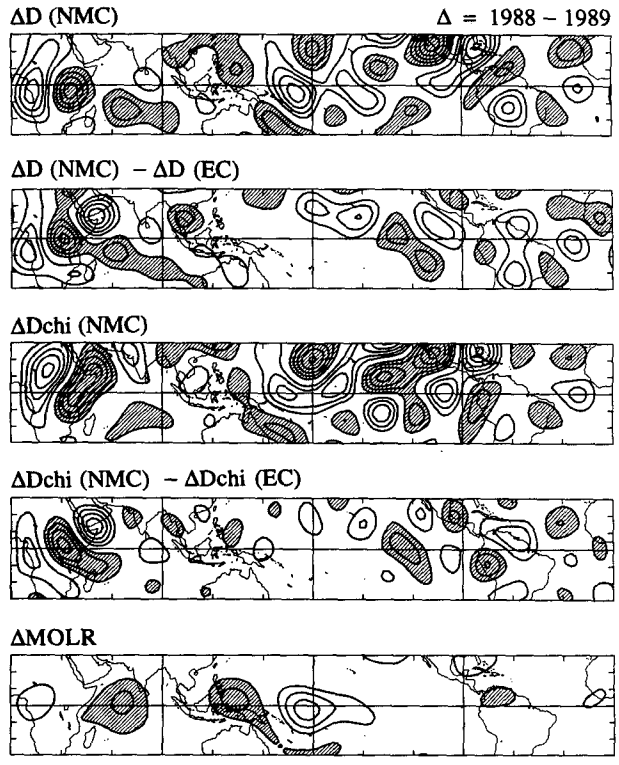

FIG. 6. As in Fig. 5 except for the January 1988 minus January 1989 difference.

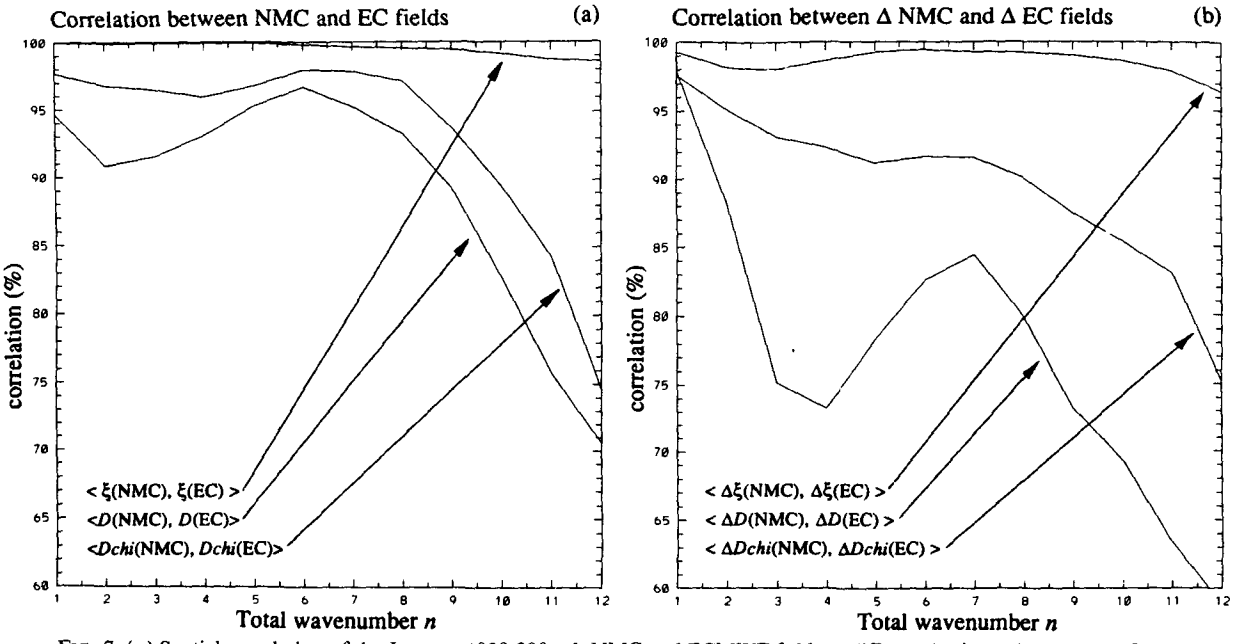

FIG. 7. (a) Spatial correlation of the January 1988 200-mb NMC and ECMWF fields at different horizontal scales as defined by the total wavenumber n. (b) As in (a) but for the difference fields January 1988 minus January 1989.

The agreement between ΔD and $\Delta Dchi$ itself is much better than that between either and ΔMOLR. Some structures are more believable in the $\Delta Dchi$ field. For example, ΔD(NMC) indicates anomalous convergence over the central North Pacific, but there is a large discrepancy between the NMC and EC estimates here as indicated by the similar magnitude of ΔD(NMC) $- \Delta D$(EC). The $\Delta Dchi$(NMC) field also shows anomalous convergence in this region, but now the NMC and EC estimates are more consistent, as seen in the plot of $\Delta Dchi$(NMC) $- \Delta Dchi$(EC). (Interestingly, the ΔMOLR field also indicates anomalous convergence in this region, but the magnitude is much too weak.) Similar statements can be made about the anomalous divergence over west-central Africa, the anomalous convergence southeast of Hawaii, and the anomalous divergence over the equatorial Atlantic. In regions where the NMC and EC fields are already consistent, the chi problem solutions generally do not degrade that consistency.

Our assertions concerning the greater consistency of the chi problem solutions can perhaps be judged more objectively by examining the spatial correlations of the NMC and EC vorticity fields, NMC and EC divergence fields, NMC and EC chi problem solutions, etc. We do this in Figs. 7a and 7b, where we show these correlations as a function of the horizontal scale. Looking at the correlations of the 1988 fields in Fig. 7a, we see that the NMC and EC vorticity fields are correlated at more than the 98% level down to wavenumber 12. The analyzed divergence fields D are less well correlated, with the values dropping to 70% at $n = 12$. The chi problem solutions $\Delta Dchi$ are somewhat better correlated than this. Note that the $\langle Dchi$(NMC), $Dchi$(EC)$\rangle$ correlation does not attain the high values of the $\langle \xi$(NMC), ξ(EC)$\rangle$ correlation. This is because what is relevant in Eq. (1) are combinations of the streamfunction gradients, not vorticity itself, and these are less well correlated than vorticity.

Figure 7b shows the consistency of the Δ fields. The $\langle \Delta\xi$(NMC), $\Delta\xi$(EC)$\rangle$ correlation remains at the high values of ~98%, but the $\langle \Delta D$(NMC), ΔD(EC)$\rangle$ correlation drops to 60% by wavenumber 12. The consistency of the chi problem solutions is considerably higher, with the $\langle \Delta Dchi$(NMC), $\Delta Dchi$(EC)$\rangle$ correlation remaining at the ~75% level even at wavenumber 12.

A final view of the improvement made by solving the chi problem is given in Table 1, which summarizes the information contained in Figs. 1–2 and 4–6. The numbers in the first column of the table show the rms of the values on these maps from 30°N to 30°S. If one interprets the rms of the NMC fields as the "signal" and the rms of the NMC–EC fields as "noise," then one can divide one by the other and call it a signal-to-noise ratio. These ratios are shown in column 2. The ratio is high for ξ and $\Delta\xi$, small for D, and even smaller for ΔD. Applying the chi problem technique nearly doubles the signal-to-noise ratio both for the divergence field and its interannual change.

5. Estimates of the mean meridional circulation

Our statements concerning the estimates of the 200-mb divergence apply equally well to estimates of the mean meridional wind V. These estimates are displayed in Fig. 8. In all four panels the discrepancy NMC–EC between the NMC and EC derived quantities is given

TABLE 1. The root-mean-square (rms) of the values in Figs. 1, 2, 4, 5, and 6 computed in the latitude belt 30°N–30°S. The values in the second column show the signal-to-noise ratios as defined in the text.

	Rms value	Signal-to-noise ratio
ξ(NMC)	17.1×10^{-6} s^{-1}	
ξ(NMC) − ξ(EC)	1.1×10^{-6} s^{-1}	17.9
$\Delta\xi$(NMC)	13.4×10^{-6} s^{-1}	
$\Delta\xi$(NMC) − $\Delta\xi$(EC)	0.9×10^{-6} s^{-1}	14.2
C(NMC)	42.4×10^{-11} s^{-2}	
C100(NMC)	2.1×10^{-11} s^{-2}	
C(EC)	40.9×10^{-11} s^{-2}	
C100(EC)	2.0×10^{-11} s^{-2}	
D(NMC)	10.1×10^{-7} s^{-1}	
D(NMC) − D(EC)	4.7×10^{-7} s^{-1}	2.1
Dchi(NMC)	10.8×10^{-7} s^{-1}	
Dchi(NMC) − *Dchi*(EC)	2.8×10^{-7} s^{-1}	3.8
ΔD(NMC)	9.1×10^{-7} s^{-1}	
ΔD(NMC) − ΔD(EC)	5.4×10^{-7} s^{-1}	1.7
Δ*Dchi*(NMC)	10.9×10^{-7} s^{-1}	
Δ*Dchi*(NMC) − Δ*Dchi*(EC)	3.4×10^{-7} s^{-1}	3.2

by the light curves. The full EC fields can be obtained by subtracting the light curves from the dark curves.

The dark curve in Fig. 8a shows V(NMC), the January 1988 mean meridional wind at 200 mb. The upper branches of the Hadley and Ferrel cells are evident in both hemispheres. The discrepancy between the NMC and EC estimates is, however, is as large as 0.4 m s^{-1} at some latitudes. The EC analyses indicate a somewhat weaker Northern Hemisphere (NH) Hadley cell and substantially different Ferrel cells in both hemispheres.

The chi problem solutions are shown in Fig. 8b. The discrepancy between the NMC and EC estimates is now smaller, of order 0.2 m s^{-1}. The plot of *Vchi*(NMC) indicates a weaker NH Hadley cell than V(NMC), a stronger NH Ferrel cell, and a weaker SH Ferrel cell. The difference V − *Vchi* (not shown) is smaller for the EC than for the NMC analyses; thus, the EC-analyzed mean meridional flow is dynamically more consistent with a frictionless zonal mean momentum budget.

Figures 8c and 8d show estimates of the change Δ between January 1988 and January 1989 in a similar

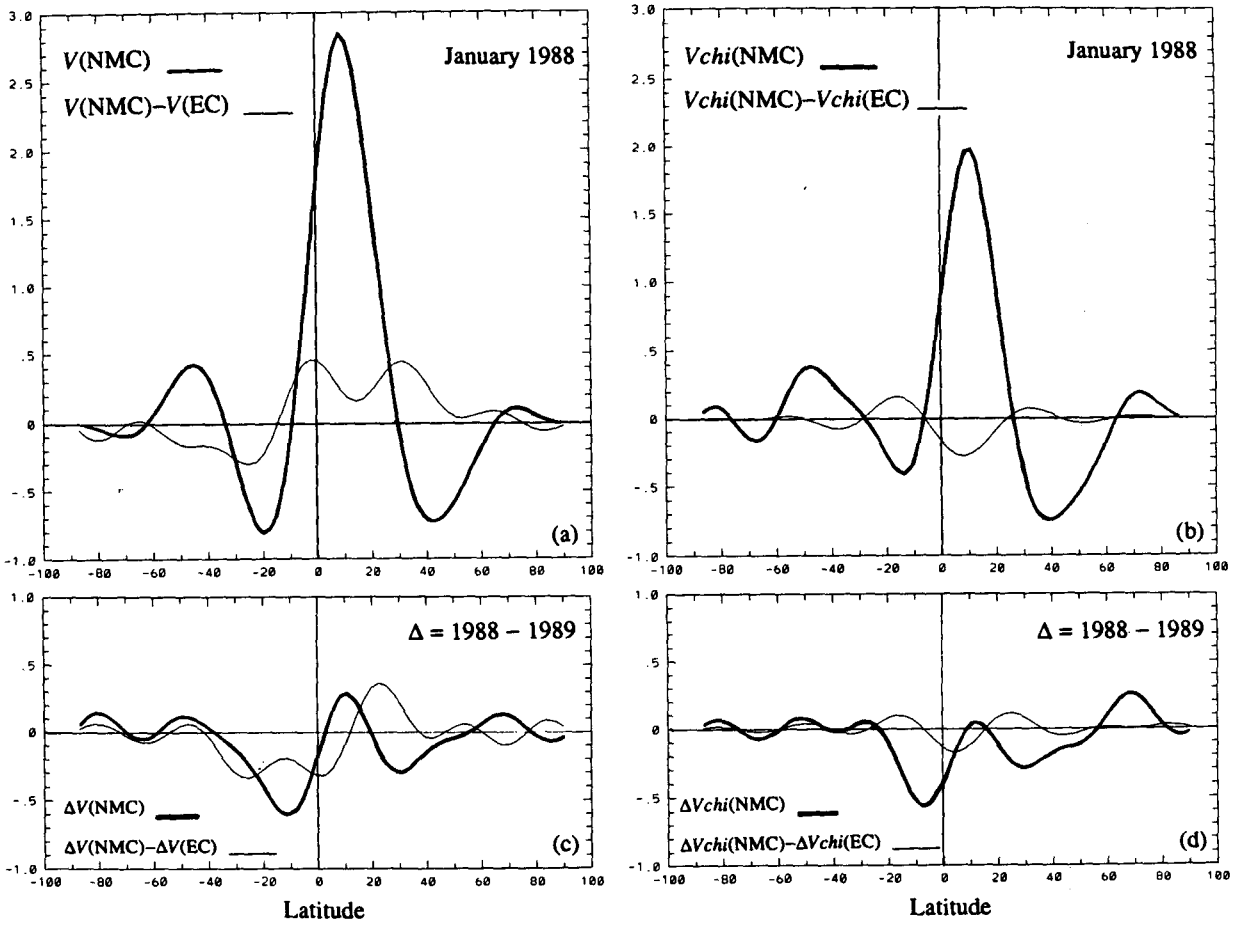

FIG. 8. (a) Dark curve: the January 1988 mean zonal mean meridional flow V at 200 mb as estimated by NMC. Light curve: the difference NMC minus ECMWF of the same quantity. (b) As in (a) but for the chi problem solutions. (c) and (d) As in (a) and (b) but for the difference January 1988 minus January 1989. The abscissa in all the plots is degrees latitude and the ordinate is m s^{-1}.

format. It is clear from Fig. 8c that the discrepancy between the NMC and EC analyzed estimates is of the same order as the change itself. The discrepancy between the chi problem estimates, given by the light curve in Fig. 8d, is significantly smaller.

6. Summary and discussion

In this paper we compared the NMC and ECMWF monthly mean analyses of the 200-mb flow with special emphasis on the tropics. January 1988 and January 1989 were chosen for detailed study. Our main interest was in determining if the analyses provided a consistent description of the flow in these two months and also of the difference between them. It was found that the analyses of the rotational component of the flow were more consistent than the analyses of the divergent component. The divergence analyses provided especially inconsistent estimates of the difference between the two months. We then sought to improve upon this situation by deriving divergence fields from the vorticity budget, hoping to exploit the more reliable analyses of the rotational flow, and we obtained encouraging results in many regions. Mo and Rasmusson (1993) have recently applied the original version of this technique to study the 1986–1989 ENSO cycle.

In data-sparse areas, the analyses rely heavily upon model forecasts to provide first-guess fields. These forecasts are obviously different because the initial states for them are different and because the models are different. The tropical forecasts are especially sensitive to the parameterization of deep convection in the model. This strongly influences the first guess of both the upper-level vorticity and the upper-level divergence. The job of the analysis is to correct these guesses using the available observations. In data-void regions, there is no alternative but to retain the guess as the "analysis." Even in areas with data, the schemes typically respond better to the rotational than to the divergent flow information in the observations, and different analysis schemes do this differently. In effect, the schemes are more efficient at correcting a model-generated vorticity guess than a model-generated divergence guess. Daley (1985) examined the spectral characteristics of the ECMWF scheme and showed that it severely attenuated the divergent flow information in the observations even on very large scales. In fact, until 1989 the scheme did not correct the first-guess divergence on the scale of the analysis box ($\sim$600 km) at all. Unden (1989) has recently introduced modifications to deal with this problem.

Data assimilation systems at operational forecasting centers are continually undergoing improvement. Ironically, the improvements made over several years introduce a spurious interannual variability in the analyses. A major reanalysis of the past data with the latest and most advanced techniques has been proposed to deal with this problem and is already under way at several centers.

One should bear in mind, however, that the performance of any data assimilation system is ultimately limited by the availability and the quality of the raw observations. Discrepancies between the analyses produced at different centers are largest in data-sparse areas. Unless the reanalyses are able to utilize more observations in these areas than previously, they will not necessarily lead to more consistent results. Even in cases where the data volumes are enormously inflated, as in 1979, the data from different observing platforms are of sufficiently different quality (see Hollingsworth et al. 1989) that different weights assigned to them at different centers would lead to inconsistent analyses. These would, of course, be within the range of observational uncertainty, but the real question is how to proceed if that range is of the same order as interannual change.

We propose to extend our work in two different directions. One is to relax the assumption that there are no errors in the rotational flow. We hope that this will lead to further improvement in the consistency of our chi problem solutions, especially over Africa. The vorticity balance there is delicate in the sense that the small errors in the vorticity are relatively more important than elsewhere. Our second extension is to perform multilevel calculations, including the vertical advection and twisting terms and also the frictional formulations incorporated in sophisticated general circulation models. We then intend to use the three-dimensional distribution of the horizontally divergent flow and the associated vertical motion thus obtained to estimate the diabatic heating rate as a balance requirement in the heat budget. The method is discussed in detail in a companion paper by Sardeshmukh (1993).

Acknowledgments. We thank NMC and ECMWF for making their circulation analyses available. This research was supported in part by a grant from the Office of Global Programs. We thank David Battisti for his comments on an earlier version of this paper.

REFERENCES

Daley, R., 1985: The analysis of synoptic scale divergence by a statistical interpolation procedure. *Mon. Wea. Rev.*, **113**, 1066–1079.

Hollingsworth, A., J. Horn, and S. Uppala, 1989: Verification of FGGE assimilations of the tropical wind field: The effect of model and data bias. *Mon. Wea. Rev.*, **117**, 1017–1038.

Julian, P. R., 1984: Objective analysis in the tropics: A proposed scheme. *Mon. Wea. Rev.*, **112**, 1752–1767.

Mo, K., and E. M. Rasmusson, 1993: The 200-mb Climatological Vorticity Budget during 1986–1989 as Revealed by NMC Analyses. *J. Climate*, **6**, 577–594.

Sardeshmukh, P. D., 1993: The baroclinic chi problem and its application to the diagnosis of atmospheric heating rates. *J. Atmos. Sci.*, **50**, 1099–1112.

——, and B. J. Hoskins, 1987: On the derivation of the divergent flow from the rotational flow: The chi problem. *Quart. J. R. Meteor. Soc.*, **113**, 339–360.

Unden, P., 1989: Tropical data assimilation and analysis of divergence. *Mon. Wea. Rev.*, **117**, 2495–2517.